Electronic Supplementary Information

Chemical Communications

Feasible polarised white-light emission based on conjugate plane structured yellow/blue dye molecules encapsulated in metal-organic frameworks

Jin Wang,*[a] Huiqing Hu,[a] Xiaoli Liu,[a] Minxiang Zhou,[a] Yunqing Lu [a] and Xinhui Zhou [b]

[a] *School of Telecommunication and Information Engineering, Nanjing University of Posts and Telecommunications, Nanjing 210003, China*

[b] *Key Laboratory for Organic Electronics and Information Displays & Institute of Advanced Materials, Nanjing University of Posts & Telecommunications, Nanjing 210023, China*

*Corresponding authors.

E-mail: jinwang@njupt.edu.cn.

Experimental Section

Synthesis of MOF crystal

The synthesis of MOF was based on the solvent-thermal reaction. The detailed synthesis steps were as follows: a mixture of $Zn(NO_3)_2 \cdot 6(H_2O)$ (2.8 mmol), Bipheny-4,4'-dicarboxylic Acid (H_2BPDC) (2.9mmol), Tirethylene diamine (TED) (1.95 mmol) was added to a 30 ml N,N-Dimethylformamide (DMF) solution; an ultrasonic treatment was applied to dissolve all chemicals until the solution was clear; afterwards, a nitric acid solution was added to the solution to adjust the pH value. The solution was then transferred into a 50 ml Teflon-lined autoclave with a stainless steel protective sleeve and heated in an oven at 120 °C for 48 h. Finally, after being cooled naturally to the room temperature, colourless transparent millimetre sized MOF crystals were obtained. Based on $Zn(NO_3)_2 \cdot 6(H_2O)$, the molar mass of MOF was 552.36 g/mol, and the yield of MOF was 57.2%.

Synthesis of MOF⊃dyes crystal

The synthesis steps of MOF⊃KSN (fluorescent brightener) crystals were as follows: a mixture of $Zn(NO_3)_2 \cdot 6(H_2O)$ (2.8 mmol), H_2BPDC (2.9 mmol), and TED (1.95 mmol) was added to a 30 ml DMF solution; an ultrasonic treatment was applied to dissolve all the chemicals until the solution was clear; afterwards, a nitric acid solution was added to the solution to adjust the pH

value, and the MOF precursor solution was obtained. Then, 30 mg of KSN were added into a precursor solution (30 ml) and ultra-sonicated until the KSN was completely dissolved to produce the MOF solution with KSN. The samples were transferred to a 50 ml Teflon-lined autoclave with a stainless steel protective sleeve and heated in an oven at 120 °C for 48 h, the reaction stopped after the samples were cooled naturally to the room temperature. The MOF⊃KSN crystal was obtained after the product was cleaned by using the DMF solvent and no fluorescence in the detection spectrum under the ultraviolet lamp of the fluorescence detection system. For the MOF⊃RhB crystal, most of the synthesis steps were the same as those of the MOF⊃KSN, except the RhB of the same quality was used.

Synthesis of MOF⊃KSN/RhB

The synthesis steps of MOF⊃KSN/RhB crystal via hierarchically growth method via two stages. First, the MOF⊃KSN crystals were in-situ synthesized in a MOF precursor solution with the KSN molecules, where the detailed procedure was the same as that of the previous section. Then, the washed MOF⊃KSN crystals were immersed in a new MOF precursor solution with the RhB molecules. In this stage, due to the presence of the MOF⊃KSN crystals, the MOF building units and guest RhB molecules were preferentially in-situ

assembled on the MOF⊃KSN crystals, and finally the MOF⊃KSN/RhB crystals were formed.

Characterisation

For material characterisation, single crystal X-ray Diffraction (XRD) was carried out with X-ray powder diffractometer (BRUKER D8-Quest). The molecular structure diagrams of the MOF crystal were obtained from single crystal XRD experimental data. Powder X-ray diffraction (PXRD) patterns were collected in the 2θ = 5−50° range on Bruker D8-Advanced-A25 diffractometer with Cu Kα radiation (λ = 1.541 Å) at 40 kV and 40 mA. N_2 adsorption-desorption isotherms were measured using V-SORB 2800P specific surface area and aperture analyser at 77K. Absolute fluorescence quantum yield was obtained by using the calibrated integrating sphere system.

The photoluminescence (PL) spectra of the MOF⊃KSN/RhB crystal was measured with a modified fluorescence polarisation measurement system (Shimadzu RF-6000 Plus Fluorescence Spectrophotometer), shown in Figure S2. The measurement system consisted of a light source, the sample, a polariser for determining the direction of polarisation, and a detector. The light source emitted a 365 nm monochromatic light that excited the sample. The polariser was placed vertically to the *x*-axis, namely the transmission direction. When the transmittance axis of the polariser was aligned along the *y*-axis, it was also in

parallel to the direction of the MOF⊃dye channel. Under such conditions, the detected light intensity was recorded as $I_{//}^{\mathrm{em}}$. When the transmittance axis of the polariser was along the *z*-axis and thus perpendicular to the direction of the MOF⊃dye channel, a new light intensity was recorded as $I_{/\perp}^{\mathrm{em}}$. The fluorescence polarisation characteristics of the material can be described by the polarisation ratio, whose definition is given as [S1]

$$P_{\mathrm{em}} = \frac{I_{//}^{\mathrm{em}}}{I_{\perp}^{\mathrm{em}}} \tag{S1}$$

Supplementary Figures

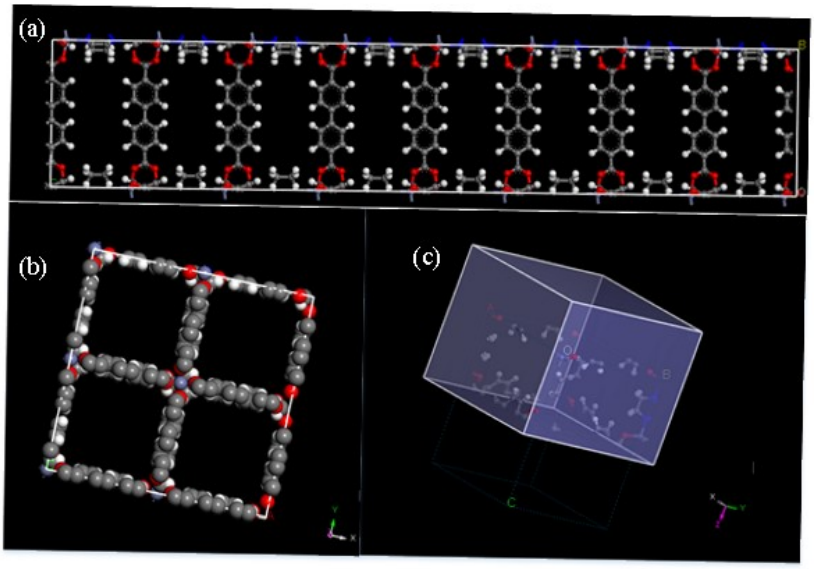

Figure S1. (a) Side and (b) cross sectional view of the molecule structure of the MOF crystal, which shows that the MOF crystal has a periodical channel structure along the c-axis; (c) Morphology illustration of MOF crystal, simulated by the Bravais-Friedel-Donnay-Harker (BFDH) method, and the c-axis direction of the crystal structure is the direction of the macroscopic quadrilateral crystal axis.

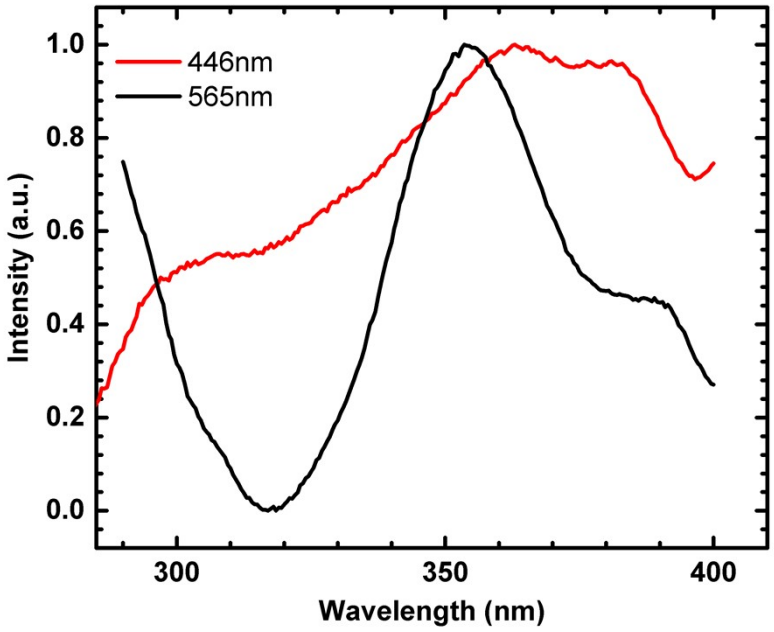

Figure S2. The excitation spectra of the MOF⊃KSN/RhB crystal at the emission wavelengths of 446 nm and 556 nm.

From the measured excitation spectra of the MOF⊃KSN/RhB crystal at the emission wavelengths of 446 nm and 556 nm, the optimal excitation wavelength is around 365 nm.

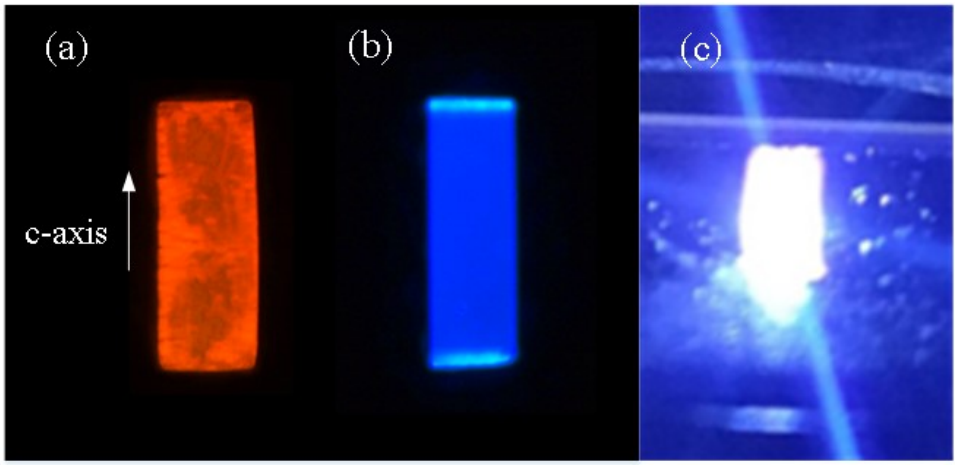

Figure S3. Microscopic images of fluorescent (a) MOF⊃RhB, (b) MOF⊃KSN and (c) MOF⊃KSN/RhB under an excitation light at a wavelength of 400 nm.

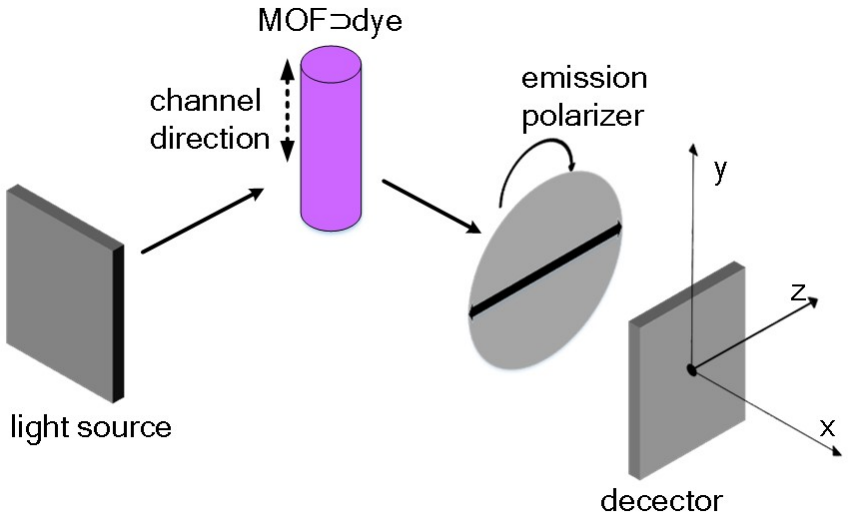

Figure S4. Scheme for characterizing the polarisability of the fluorescence spectra of the MOF⊃dye crystal. The local coordinate systems are defined with respect to the transmission direction.

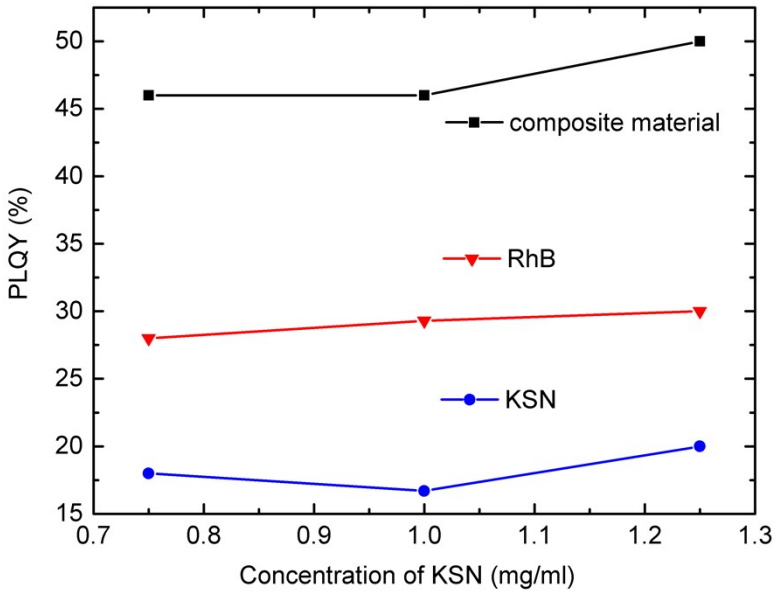

Figure S5. Quantum yield diagram of MOF coated KSN, RhB and KSN/RhB (composite material) in MOF⊃KSN/RhB in crystal state.

This shows that the quantum yield of MOF⊃KSN/RhB in crystal state can reach 50%, in which KSN and RhB contribute about 20% and 30% respectively. However, the quantum yields of KSN and RhB were not significantly affected with the increase of KSN concentration from 0.75 mg/ml to 1.25 mg/ml.

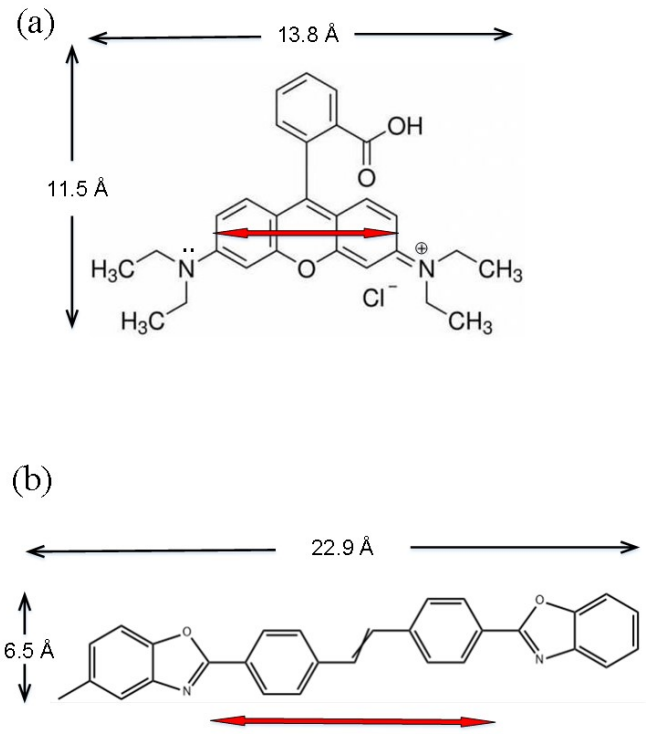

Figure S6. The molecular structure diagram of (a) RhB and (b) KSN.

The RhB molecules have a rod-shaped conjugated structure, and the polarisation direction of its emitted light is consistent with the long axis direction of the rod-shaped molecules. The KSN molecules also have a linear conjugated planar structure.

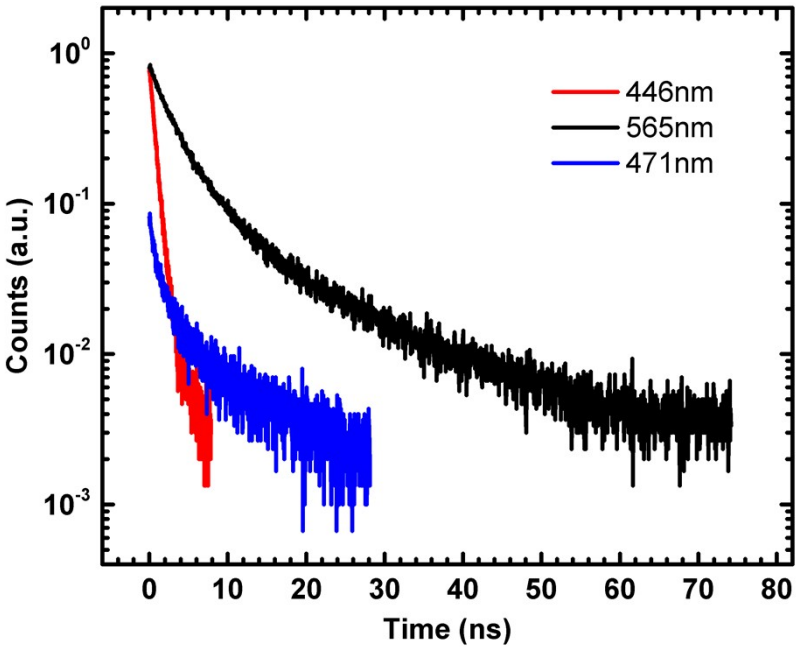

Figure S7. Fluorescence decay curves of MOF⊃KSN/RhB in the solid state at room temperature, monitored at 446nm, 471nm and 565nm with λ_{ex} = 365nm.

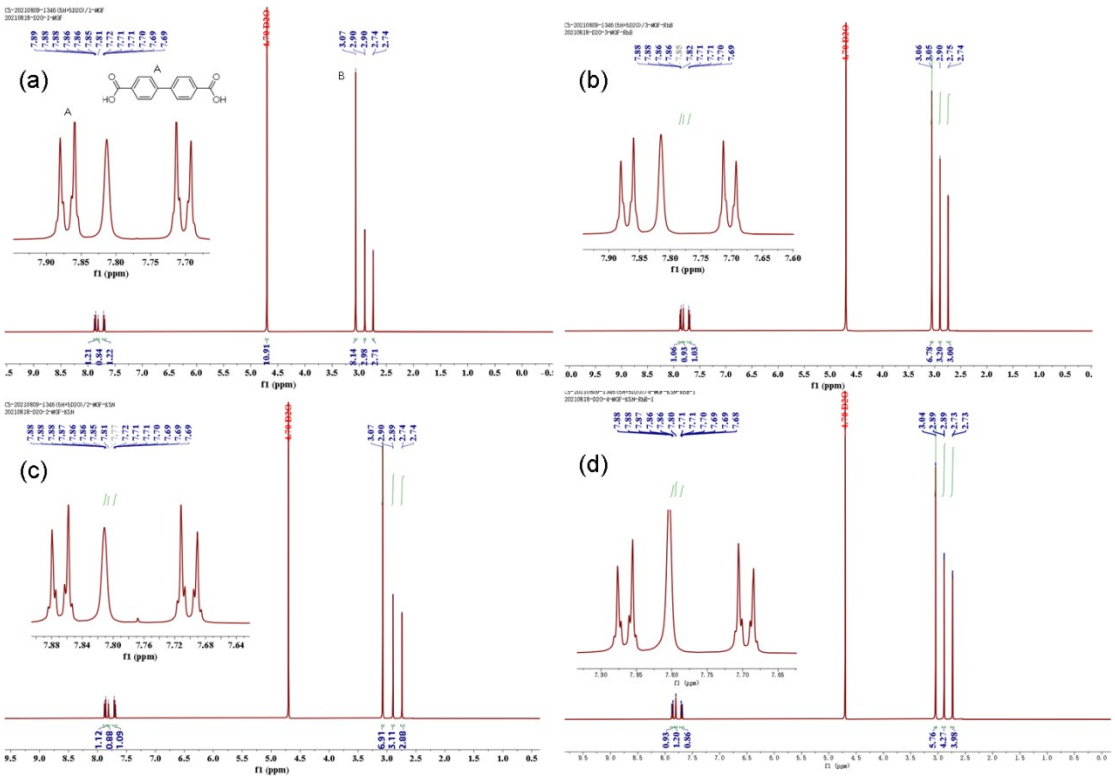

Figure S8. The ^{1}H NMR spectra of (a) MOF, (b) MOF⊃RhB , (c) MOF⊃KSN and (d) MOF⊃KSN/RhB after outgassing at 100°C for one hour under house vacuum.

MOF：^{1}H NMR (400 MHz, D2O) δ 7.87 (d, J = 8.4 Hz, 1H, H_2BPDC), 7.81 (s, 1H, CH, in DMF), 7.70 (d, J = 8.4 Hz, 1H, H_2BPDC), 3.07 (s, 8H, NCH_3, in DMF), 2.90 (s, 3H, NCH_3, in DMF), 2.74 (s, 3H, TED).

MOF⊃RhB：^{1}H NMR (400 MHz, Deuterium Oxide) δ 7.91 – 7.84 (m, 1H), 7.82 (s, 1H), 7.74 – 7.66 (m, 1H), 3.05 (d, J = 0.9 Hz, 7H), 2.90 (s, 3H), 2.74 (d, J = 0.8 Hz, 3H).

MOF⊃KSN：^{1}H NMR (400 MHz, Deuterium Oxide) δ 7.91 – 7.83 (m, 1H), 7.81 (s, 1H), 7.74 – 7.66 (m, 1H), 3.07 (s, 7H), 2.90 (d, *J* = 0.6 Hz, 3H), 2.74 (d, *J* = 0.8 Hz, 3H).

MOF⊃KSN/RhB：^{1}H NMR (400 MHz, Deuterium Oxide) δ 7.90 – 7.83 (m, 1H), 7.80 (s, 1H), 7.73 – 7.66 (m, 1H), 3.04 (s, 6H), 2.89 (d, J = 0.6 Hz, 4H), 2.73 (d, J = 0.8 Hz, 4H).

In the NMR of MOF, it was confirmed that a certain amount of DMF remained in the channel. After the introduction of KSN and RhB, the peak integral intensity of DMF decreased in proportion. Therefore, the molecular content of fluorophores in MOF⊃KSN and MOF⊃RhB can be preliminarily determined by the proportion of DMF reduction in ^{1}H NMR. The unit cell volume of MOF is V=2241.7Å^3, and each unit cell has two secondary building units, namely an average of two H_2BPDC ions are contained in each unit cell. So, the concentration of H_2BPDC in the MOF is 1.48 mmol/cm^3. Since there is only one hydrogen on the position A related to DMF and three hydrogens on the position B related to H_2BPDC, the molecular number ratio between DMF and H_2BPDC can be calculated as n_{DMF}/m_{H2BPDC} = (8/3)/1.00 can be obtained, where n_{DMF} and m_{H2BPDC} are the number of respective molecule. So, in MOF, the concentration of DMF in the MOF is 3.95 mmol/cm^3. In the MOF⊃RhB and MOF⊃KSN crystal, n_{DMF}/m_{H2BPDC} are (7/3)/1.00 and (7/3)/1.00, respectively. Then the concentration of DMF in each crystal is 3.45 mmol/cm^3 and 3.45 mmol/cm^3. It can also be obtained that the concentration of RhB and KSN in each crystal are 0.50 mmol/cm^3 and 0.50 mmol/cm^3 respectively. The molecular weight of MOF is 552.36

g/mol, so the mass fractions of RhB and KSN in MOF⊃RhB and MOF⊃KSN are 10.48wt% and 9.49wt%, respectively. However, the ratio of KSN to RhB in MOF⊃KSN/RhB is difficult to obtain directly. So, it is difficult to obtain their respective mass fractions.

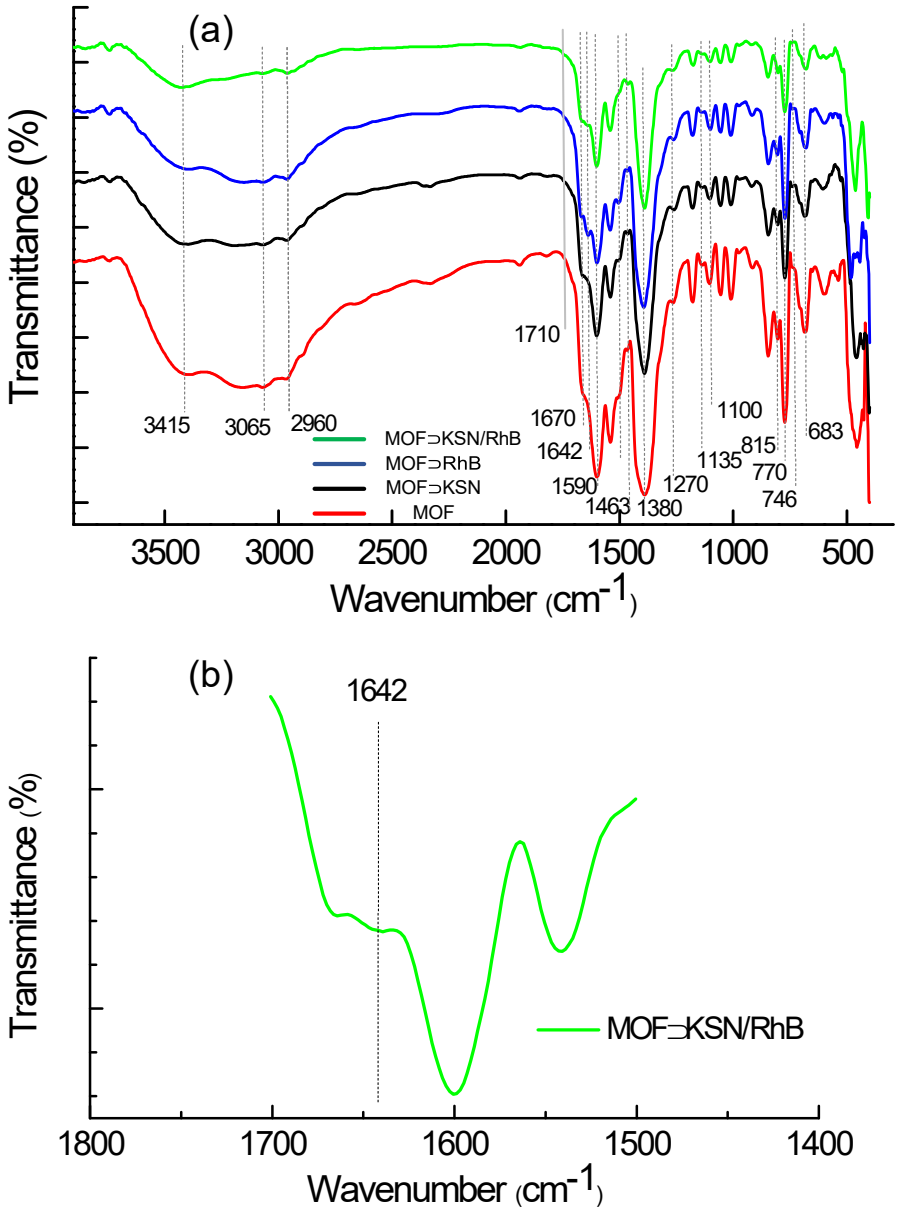

Figure S9. The FTIR spectra of (a) MOF (red), MOF⊃KSN (black) MOF⊃RhB (blue) and MOF⊃KSN/RhB (green); (b) the zoomed FTIR spectrum of MOF⊃KSN/RhB.

When fluorescent molecules were introduced into MOF channels, the overall vibration intensity of FTIR decreased. In the FTIR of MOF, the wide intensity band at 3415 cm^{-1} is related to the O-H stretching vibration of hydroxyl, the strong vibration at 1380 cm^{-1} is related to the C-H vibration of CH_3, and their occurrence is related to

the undischarged water and DMF in the channel; a weak intensity band of 3065 cm^{-1} belongs to aromatic C-H vibration. It also exists at 1135 cm^{-1} (plane bending), 815 cm^{-1} (out of plane bending) and 683 cm^{-1} (swing vibration). An obvious absorption band appears at 1590 cm^{-1}, which is due to the asymmetric stretching vibration of -COO group. The vibration at 1463 cm cm^{-1} further confirms this point. These fluctuations are related to H_2BPDC. The sharp peak of 770 cm^{-1} is related to the C-H vibration of CH_2, and this fluctuation is related to TED.

The binding sites of RhB and KSN with MOF were further deduced by FTIR. In the spectra of MOF⊃RhB and MOF⊃KSN/RhB, the band (Figure S9(b)) at position 1642 cm^{-1} associated with the C=N stretching vibreation indicates the presence of RhB. At 1590 cm^{-1}, the vibration from the COO- group still exists, but the strong band of the OH^- group does not appear around 3300 cm^{-1}. It can be speculated that RhB is coordinated with the metal site of MOF through carboxyl dehydrogenation. In the spectra of MOF⊃KSN and MOF⊃KSN/RhB, it can be confirmed that the bands at 1463 cm^{-1} and 746 cm^{-1} (the C—H out-of-plane deformation vibration on the benzoxazole ring) are related to the benzoxazole ring, which indicates the existence of KSN. Since the strong sharp peak of CH_3 does not appear near 2900 cm^{-1}, and the hydrogen atom connected to the benzene ring is more active, it is speculated that KSN is coordinated with the metal site of MOF through methyl dehydrogenation.

Table S1. Fitted parameters for PL time decays excited at 365 nm, for (1) and (2) MOF⊃KSN with the KSN concentration of 1.0 ml, (3) MOF⊃RhB with the RhB concentration of 2.0 ml, and (4), (5), (6) MOF⊃KSN/RhB with the KSN concentration of 1.0 ml and the RhB concentration of 2.0 ml.

	τ_1 (ns)	τ_2 (ns)	τ_{avg} (ns)[a]
MOF⊃KSN (λ_{em} = 446 nm)	0.64	4.35	0.67
MOF⊃KSN (λ_{em} = 471 nm	1.69	10.68	10.07
MOF⊃RhB (λ_{em} = 565 nm)	3.02	12.87	6.90
MOF⊃KSN/RhB (λ_{em} = 446 nm)	0.68	5.78	0.72
MOF⊃KSN/RhB (λ_{em} = 471 nm)	0.79	5.51	4.42
MOF⊃KSN/RhB (λ_{em} = 565 nm)	3.29	9.92	7.49

Average fluorescence lifetimes calculated by equation $\tau_{avg} = A_1\tau_1 + A_2\tau_2$.[S8]

Table S2. Optical properties of dyes dissolved in the DMF solution or encapsulated in MOF under a light excitation at 365 nm.

Sample	DMF Solution			Monocrystal		
	λ_{em} (nm)	Quantum yield (%)	τ_{avg} (ns)	λ_{em} (nm)	Quantum yield (%)	τ_{avg} (ns)
KSN	443	N/A	N/A	446/471	N/A	0.67/10.07
RhB	570	<1	2.41	565	20	6.90
KSN/RhB	443/570	2.1	N/A	446/565	50	0.72/7.49

Table S3. CIE coordinates of the MOF⊃KSN/RhB crystal for different angles of the polariser.

Angle (°)	CIE
0	(0.2912, 0.2363)
15	(0.3292, 0.2683)
30	(0.3432, 0.2735)
45	(0.355, 0.2923)
60	(0.3608, 0.2761)
75	(0.3851, 0.3084)
90	(0.3726, 0.3186)
105	(0.3711, 0.3108)
120	(0.3725, 0.2922)
135	(0.3683, 0.2882)
150	(0.3405, 0.2811)
165	(0.3254, 0.2612)
180	(0.3001, 0.2399)

Table S4. Optical properties of white light-emission materials containing RhB chromophore

Materials	CIE	PLQY (%)	τ_{avg} (ns)	Polarization ratio
This article	(0.32,0.32)	60	6.90	2.98[a]
MOF 1⊃RhB[S2]	(0.33,0.33)	59.4	N/A	7.22[b]
L/D-CMOF⊃chromophores[S3]	(0.33,0.32)	66	1.25	N/A
NP4C[S4]	(0.30,0.33)	N/A	N/A	N/A
P2[S5]	(0.31,0.33)	27.2	580	N/A
W-gel[S6]	(0.31,0.36)	27	3.81	N/A
N-GOD-RhB[S7]	(0.30,0.34)	34	7.58	N/A
Ga_2O_3−RhB[S8]	(0.33,0.33)	30	3.6	N/A

[a] linear polarization；
[b] circular polarization：emission dichroic ratio.

References

S1 Y. Wang, J. Shi, J. Chen, Recent progress in luminescent liquid crystal materials: design, properties and application for linearly polarised emission. *J. Mater. Chem. C.*, 3(31): 7993-8005, 2015.

S2 H. R. Fu, N. Wang, X. X. Wu, Circularly Polarized Room-Temperature Phosphorescence and Encapsulation Engineering for MOF-Based Fluorescent/Phosphorescent White Light-Emitting Devices. Adv. Opt. Mater., 8(13): 2000330, 2020.

S3 C. Zhang, Z. P. Yan, X. Y. Dong, Enantiomeric MOF crystals using helical channels as palettes with bright white circularly polarized luminescence. *Adv. Mater.*, 32(38): 2002914, 2020.

S4 D. Li, W. Hu, J. Wang, White-light emission from a single organic compound with unique self-folded conformation and multistimuli responsiveness. *Chem. Sci.*, 9(26): 5709-5715, 2018,.

S5 H. Gui, Z. Huang, Z. Yuan, Ambient White-Light Afterglow Emission Based on Triplet-to-Singlet Förster Resonance Energy Transfer. *CCS Chemistry*, 481-489, 2021.

S6 P. Bairi, B. Roy, P. Chakraborty, Co-assembled white-light-emitting hydrogel of melamine. *ACS Appl. Mater. Interfaces*, 5(12): 5478-5485, 2013.

S7 R. Das, S. Parveen, A. Bora, Origin of high photoluminescence yield and high SERS sensitivity of nitrogen-doped graphene quantum dots. *Carbon*, 160: 273-286，2020.

S8 T. Wang, V. Chirmanov, W. H. M. Chiu., Generating tunable white light by resonance energy transfer in transparent dye-conjugated metal oxide nanocrystals. J. Am. Chem. Soc., 135(39): 14520-14523, 2013.